Controlling Factors of Phase-shift of Fine Sediment in Large-scale Debris flows

Yuki NISHIGUCHI[1 *], Taro UCHIDA[2], Yoshifumi SATOFUKA[3], Kana NAKATANI[4] and Takahisa MIZUYAMA[4]

[1] CTI Engineering, Co., Ltd, (1047-27, Onigakubo, Tsukuba, Ibaraki, 3002651, Japan)

[2] National Institute for Land and Infrastructure Management (1 Asahi, Tsukuba, Ibaraki, 3050804, Japan)

[3] Department of Civil Engineering, Ritsumeikan University (1-1-1, Noji-higashi, Kusatsu, Shiga, 5258577, Japan)

[4] Graduate School of Agriculture, Kyoto University (Kitashirakawa, Sakyo-ku, Kyoto, 6068502, Japan)

*Corresponding author. E-mail: nishiguchi@ctie.co.jp

Our previous numerical simulation studies of the run-out and propagation processes of large-scale debris flows demonstrated the applicability of the concept wherein all sediment smaller than a given diameter (D_c) in large-scale debris flow continuously behaves like a fluid. However, these studies lacked a detailed assessment of the controlling factors of D_c. In this study, we showed that the settling velocities of the best-fit D_c were lower than both the friction velocities of the debris flow and the turbulent velocities of the interstitial water. In addition, we demonstrated that the volume concentration of fine sediment behaving like a fluid was similar for different debris flows. We considered that because both the amount of fine sediment and turbulence magnitude were sufficiently high, the fine sediment concentrations in the five studied debris flows approached the upper concentration limit.

Key words: large-scale debris flow, numerical simulation, fine sediment, phase-shift

1. INTRODUCTION

Large-scale debris flows have had serious impacts on humans. It is therefore important to identify area with a large-scale debris flow hazard. However, previous studies have shown that the commonly used debris flow numerical simulation models may not be applicable for large-scale debris flows [*Egashira and Itou,* 2004]. Accordingly, some previous studies have indicated that the fine sediment in large-scale debris flows might be considered a fluid phase rather than a solid phase [e.g., *Iverson*, 1997]. Based on this phase-shift concept, *Nishiguchi et al* [2011] defined a maximum diameter of sediments that behave like a fluid, D_c, and conducted numerical simulations for large-scale debris flows that were triggered by deep-seated rapid (catastrophic) landslides in Atsumari River, Kumamoto, Japan. They found that the phase-shift of fine sediment must be included in numerical simulation models to allow for more detailed descriptions of large-scale debris flows. Moreover, *Nishiguchi et al*. [2013] added examples of simulations (Oyouchi, Tokushima Japan, Kataino River, Miyazaki, Japan, and Funaishi River, Kagoshima, Japan) and confirmed that if we use best-fit D_c, the same numerical simulation can describe the run-out processes of several past large-scale debris flows.

However, these previous studies lacked a detailed assessment of the controlling factors of D_c. We examined additional one large-scale debris flow (Nanase valley, Miyazaki, Japan) for our simulations in this study and elucidate the controlling factors of D_c.

2. NUMERICAL SIMULATION

2.1 Phase-shift concept

Most models used to describe stony debris flows assume that they consist of both solid and fluid phases [*Takahashi,* 1977]. These models are composed of a “solid phase” of sediments exhibiting laminar flow and a “fluid phase” of interstitial water exhibiting turbulent flow. However, it has been proposed that the sediments in large-scale debris flows consist of two types (coarse sediments and fine sediments), and that the motion of fine

sediment in a debris flow is similar to that of the interstitial water [e.g., *Iverson,* 1997*; Nakagawa et al., 1998, Egashira et al.,* 1998].

Nishiguchi et al. [2011] defined a maximum diameter of sediments that behave like a fluid, D_c (Fig. 1) and assumed that all sediment smaller than D_c behaved as a fluid. Based on this phase-shift concept, they characterized the key parameters for the numerical simulation: the sediment concentration of the debris flow (C_d, Eq. 1), the interstitial fluid density of the debris flow (ρ, Eq. 2), and the representative particle diameter of the debris flow (D, Eq. 3).

$$C_d = (1-w)(1-P(D_c)) \quad (1)$$

$$\rho = \frac{w\rho_w + (1-w)\rho_s P(D_c)}{w + (1-w)P(D_c)} \quad (2)$$

$$D = d(D_c), \quad (3)$$

where $P(D_c)$ is the ratio of sediment smaller than D_c to all sediment (Fig. 1), C_d is the concentration of sediment which behaves as a solid in the debris flow. ρ_w is pure water density, ρ_s is the solid density of the sediment, $d(D_c)$ is the weighted average particle diameter greater than D_c, and w is the pure water content of the debris flow.

2.2 Simulation model

The "Kanako" numerical simulator has been used widely for a variety of objectives, particularly because of its graphical user interface [*Nakatani et al.,* 2007; 2008]. *Uchida et al.* [2013] developed a modified version of the Kanako simulator, Kanako-LS, to describe the phase-shift of the fine sediment. In the Kanako-LS, sediments can be classified into two sediment diameter groups (i.e., coarse and fine), which behave as solid and fluid phases, respectively, as described in chapter 2.1. In this study, we conducted numerical simulation for five past large-scale debris flows using Kanako-LS.

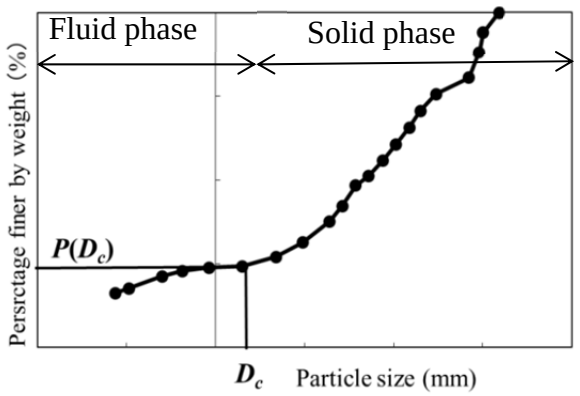

Fig.1 Conceptual diagram of the definition of D_c (after Nishiguchi et al., 2011)

Table 1 Cases for the present study

Site	Date	Total volume of debris flow at the upper end*	Travel Distance	Flow width	Maximum erosion depth
A	2003/7	31,000 m^3	1.6 km	50 m	5 m
B	2004/8	622,000 m^3	1.0 km	60 m	0 m
C	2005/9	272,000 m^3	2.1 km	40 m	0 m
D	2005/9	183, 000 m^3	0.9 km	20 m	0 m
E	2009/7	19,000 m^3	0.6 km	60 m	7 m

* including void volume

3. MATERIALS AND METHODS

3.1 Study sites

The study sites (referred to as Sites A–E) are located in Japan. These debris flows occurred between 2003 and 2009 (Table 1). All of the studied debris flows were triggered by heavy rainstorms and were caused by a deep-seated rapid landslide.

We obtained the elevations of the land surface after the debris flows from LiDAR data for Sites A–D. For Site E, we obtained the results of field survey measurements (Table 2). We obtained the elevations of the land surface before the debris flows from the topographic maps with scales of 1:2,500–1:10,000 (Table 2).The landslide volumes (including the void the volume) determined from these topographic data ranged from 1.9×10^4–6.2×10^5 m^3 and the extent of travel of the debris flow ranged from 0.6–2.1 km. Maximum erosion depths at Sites A and E were around 5 and 7 m, respectively, whereas there were no eroded areas at Sites B, C, or D. The average widths of the eroded and deposited areas at Sites A, B, C, D, and E were 50, 60, 40, 20, and 60 m, respectively. Detailed topographic information for all sites except D was reported in *Nishiguchi et al.* [2013].

We evaluated the grain size distribution of the debris flows using sieve tests, cross-sectional photographs of the deposits, and grain size distributions obtained from field measurements [*Nishiguchi et al.,* 2012](Fig. 2).

3.2 Numerical simulation method

3.2.1 Topography

The longitudinal profiles of the riverbed that we used for the numerical simulation were established based on topographic data before the debris flow events. The widths of the debris flows were determined as the averages of the riverbed widths before and after the debris flow. The initial depths of the movable bed layer were determined as the

Table 2 Sources of topographic data

Site	Topographic data		Reference about debris flow runout and diposited area
	Source of data before debris flow	Source of data after debris flow	
A	Topographic map at scale of 1:5,000	LiDAR Data(2003) (1 m mesh)	Aerial photograph
B	Topographic map at scale of 1:2,500	LiDAR Data(2004) (1 m mesh)	Literature (Hiura et al, 2004)
C	Topographic map at scale of 1:8,000	LiDAR Data(2005) (2 m mesh)	Literature (Miyazaki Prefecture, 2006)
D	Topographic map at scale of 1:8,000	LiDAR Data(2005) (2 m mesh)	Literature (Miyazaki Prefecture, 2006)
E	Topographic map at scale of 1:10,000	Field survey（2007） (40 m interval)	Literature (Kagoshima Prefecture, 2008)

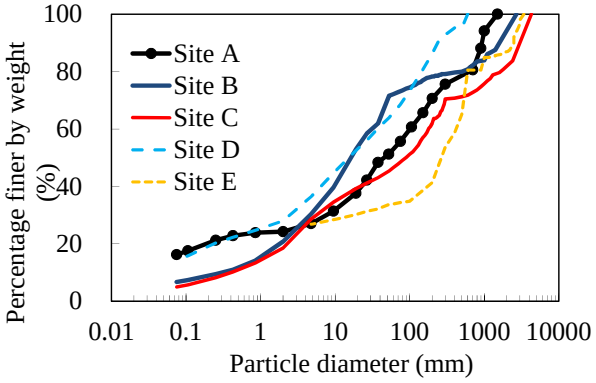

Fig. 2 Particle size distribution of debris flow (after Nishiguchi et al., 2012)

maximum erosion depth. Therefore, we set this variable to 5, 0, 0, 0, and 7 m for Sites A, B, C, D, and E, respectively.

Site E contained one grid-type sabo dam at 280 m below the landslide that was effectively blocked by the rocks and sediments of the debris flow. Therefore, we set a closed-type sabo dam in the simulation.

3.2.2 Sediment concentration at the upper end of the simulation, the representative particle diameter, and fluid density

Sediment concentration at the upper end of the simulation (i.e., the lower end of the landslide scar) and the representative particle diameter of the debris flow were determined using Eqs. 1 and 3, respectively. We assumed that w in Eq. 1 was equal to the saturated water content of the landslide mass, including both bedrock and soil. We used the porosity data collected for Site A (0.34) for all sites, because no data were available for the other sites [*Nishiguchi et al.,* 2011]. Fluid density of the debris flow was determined from Eq. 2 at each time interval according to the time variation of w in the Kanako-LS simulation.

3.2.3 Hydrograph

The process of debris flow initiation can be complex. For example, several discrete debris flows can occur in a short time (i.e., 10–100 min.). However, insufficient information about the initiation processes of debris flow meant that we assumed a single debris flow occurrence, except at Site A. *Nishiguchi et al*. [2011] showed that both muddy and stony flows occurred at Site A, and the ratio by volume of stony flow to total flow was estimated to be around 0.7. Therefore, we focused on the stony flow and assumed it to compose 70% of the total sediment volume of the debris flow. To set the input hydrograph, we used the method proposed by *Nishiguchi et al*. [2013], who assumed that the relationship between velocity and flow depth could be described by Takahashi's theory [*Takahashi*, 2004] and assumed that the longitudinal length of the debris flow was the same as that of the landslide scar. Peak discharge of hydrographs for Sites A–E were estimated as 4270, 177735, 5387, 73133, and 1758 m^3/s, respectively.

We estimated the river discharge due to rainfall by multiplying the total catchment area of the upper basin of the landslide by the highest recorded hourly amount of rainfall, or the highest recorded 10-min rainfall amount for all sites. The discharge results were 25, 83, 3, 1, and 0.5 m^3/s for Sites A, B, C, D, and E, respectively. It was determined that the river discharge for the study sites was considerably smaller than the discharge of the landslide mass flowing into the river. Therefore, we considered only the discharge of the landslide mass flowing into the river to set the hydrograph in our simulation.

3.2.4 Other properties

Parameters ρ_s and C_* were set to 2650 kg/m^3 and 0.65, respectively. We assumed that the relative proportion of fine/coarse sediments of the riverbed was equal to the relative proportion of fine/coarse sediments in the landslide mass. The values of the coefficients of the erosion and deposition rates were set to 0.0007 and 0.05, respectively, based on data from previous studies [*Nakatani et al.,* 2008*; Nakatani,* 2010].

The debris flow deposition process may be complex, because it is unclear whether fine sediment that behaves as a fluid in debris flow is deposited as a solid or as fluid [*Uchida et al*., 2013]. In the former case, the deposited layer is composed of coarse sediments and fine sediments, whereas in

the latter, the deposit is formed from coarse sediments with fluid particles deposited in the pores. Moreover, it may be possible for both processes to occur simultaneously. In this study, we assumed that fine sediment was deposited as a solid.

Nishiguichi et al. [2011; 2013] assumed that D_c was constant in both space and time, and searched for the best-fitted value of D_c for Site A, B, C, and D. In this study, we also searched the best-fitted value for Site D using the same method as the previous studies.

3.3 Verification of D_c value

For verification of our D_c value, we examined whether particles with the best-fit D_c can be physically suspended and move in a turbulent flow in the debris flow. A particle of sediment can generally be suspended in river flow if the friction velocity of the flow is larger than the settling velocity of the sediment particle size [e.g., *Ashida et al*., 1993]. Previous studies have also indicated that the energy loss due to turbulence in the interstitial flow was part of the total energy loss of the debris flow, and methods were proposed to describe the degree of turbulence of the interstitial flow as turbulent velocity [e.g., *Egashira et al*., 1994]. Therefore, we first, compared the settling velocity of the best-fit D_c and the friction velocity of the debris flow, as similar to fine sediment suspension in a river flow. We then compared the settling velocity of the best-fit D_c and the turbulent velocity of the interstitial water.

According to *Rubey* (1933), settling velocity (ω_0) can be expressed as

$$\begin{cases} \omega_0 = \sqrt{(\rho_s/\rho - 1) g d (D_c)} \cdot F(d) \\ F(d) = \sqrt{\dfrac{2}{3} + \dfrac{36\nu^2}{s g d (D_c)^3}} - \sqrt{\dfrac{36\nu^2}{s g d (D_c)^3}} \\ s = \rho_s/\rho - 1, \end{cases} \quad (4)$$

where ν is kinematic viscosity (0.01 cm^2/s).We treated ρ as the simulated mean fluid density during debris flow propagation.

The friction velocity (U^*) can be calculated from riverbed shear stress as

$$U^* = \sqrt{g h_f I_f}, \quad (5)$$

where I_f is the slope angle. We treated h_f as the simulated mean flow depth during debris flow propagation.

The turbulent velocity (v_f) can be calculated from turbulent stress [*Hotta et al*., 1998] as

$$v_f = \sqrt{\frac{\rho_f}{\rho}}, \quad (6)$$

where ρ_f is turbulent shear stress. ρ_f can be expressed as

$$\rho_f = \alpha^2 \rho \frac{25 u_f^{\,2}}{4 h_f^{\,2}} d (D_c)^2 (1 - \frac{z}{h_f}), \quad (7)$$

where u_f and h_f are simulated mean flow velocity and simulated mean flow depth of the debris flow during propagation, respectively, and z is bed elevation. The value of ρ_f averaged for flow depth (ρ_{fm}) can be expressed as

$$\rho_{fm} = \frac{\int_0^{h_f} (\alpha^2 \rho \frac{25 u_f^{\,2}}{4 h_f^{\,2}} d \ (D_c)^2 (1 - \frac{z}{h_f})) dz}{h_f}. \quad (8)$$

α can be expressed as

$$\alpha = \sqrt{k_f} \left(\frac{1 - C_{df}}{C_{df}} \right)^{1/3}, \quad (9)$$

where k_f is an empirical coefficient of 0.16 and C_{df} is the simulated mean sediment concentration during debris flow propagation.

We calculated the representative value of ω_0, U^* and v_f for five debris flow events using the best-fit D_c simulation results determined by averaging each value at the 1/4, 1/2 and 3/4 points of the debris flow travel distances, respectively.

4. RESULTS

4.1 Simulation results

The simulated travel and erosion distances matched our observations well when D_c was 15, 10, 50, 8, and 200 mm at Sites A, B, C, D, and E, respectively (Fig.3). The simulated distances and depths of erosion and deposition also agreed well with those observed, except in the upper stream at Site C. Although the calculated travel distance of the debris flow matched the observed travel distance at Site C, the deposition pattern at 0–750 m from the upper end of the calculation could not be fully described by our simulation.

4.2 Settling, friction, and turbulent velocity

The calculated results of ω_0, U^*, and v_f for five debris flows are shown in Table 3. We found that the settling velocities of the best-fit D_c ranged between 16 cm/s (Site D) and 83 cm/s (Site E). The friction velocities of the debris flow and the turbulent velocities of interstitial water were 151–392 cm/s and 25–95 cm/s, respectively. Thus, the friction velocities of the debris flow and the turbulent velocities of the interstitial water were 3–21 times and 1–4 times higher than the settling velocities of the best-fit D_c, respectively (Fig. 4).

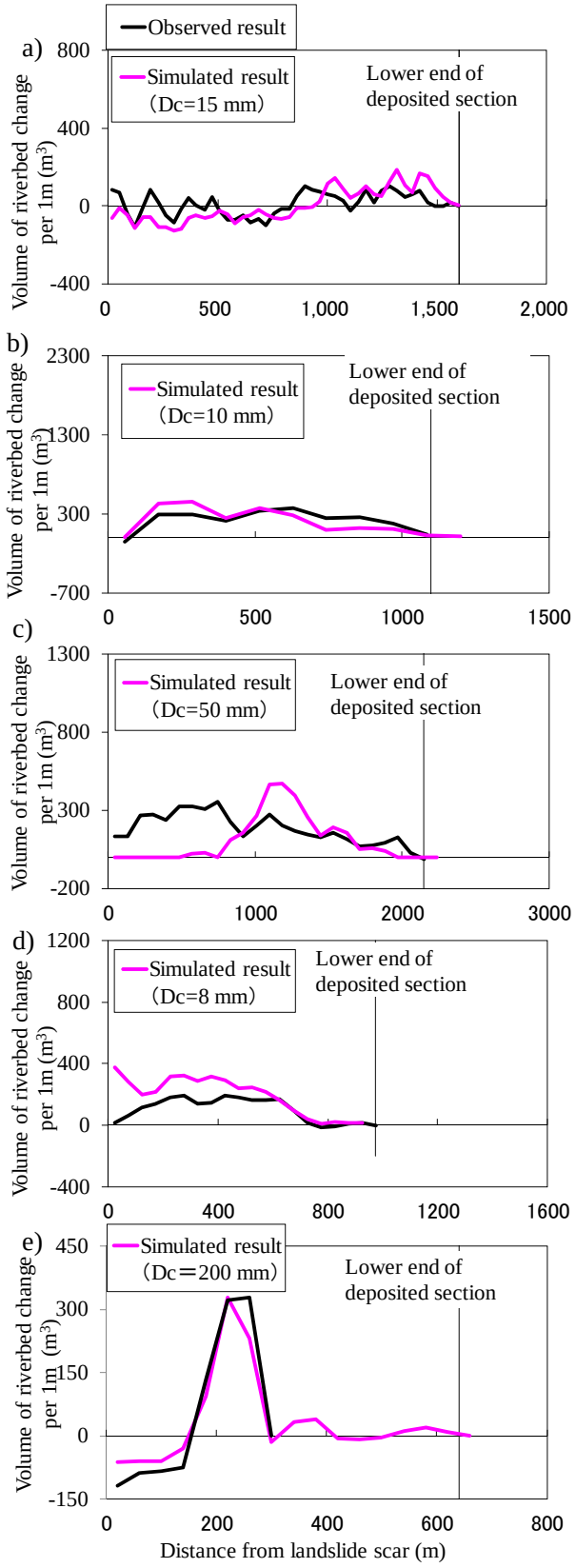

Fig.3 Simulated result of reasonable D_c and observed result at a) Site A, b) Site B, c) Site C, d) Site D, e) Site E

Table 3 Friction velocities, settling velocities, and turbulent velocities of the simulation results

Site	Friction velocity of debris flow	Settling velocity of D_c	Turbulent velocity of interstitial water
A	201 cm/s	24 cm/s	50 cm/s
B	392 cm/s	18 cm/s	71 cm/s
C	151 cm/s	39 cm/s	80 cm/s
D	256 cm/s	16 cm/s	25 cm/s
E	224 cm/s	83 cm/s	95 cm/s

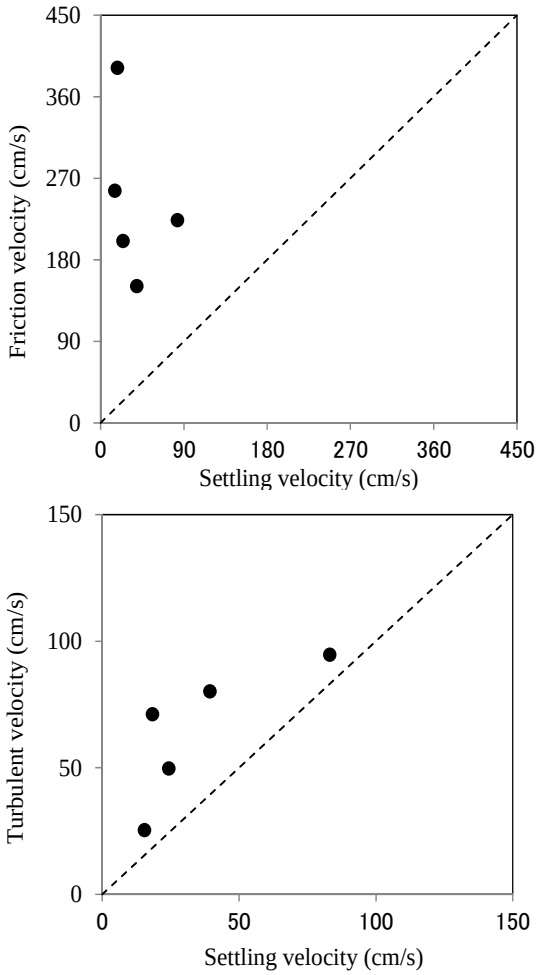

Fig.4 Relationship between settling velocity and friction velocity (upper figure), and between settling velocity and turbulent velocity (lower figure)

5. DISCUSSION

Fig 4 shows that the settling velocities of the best-fit D_c were considerably lower than both the friction velocities of the debris flow and the turbulent velocities of the interstitial water for all five debris flow events. These results suggest that sediment particles smaller than D_c can be suspended and behave as a fluid.

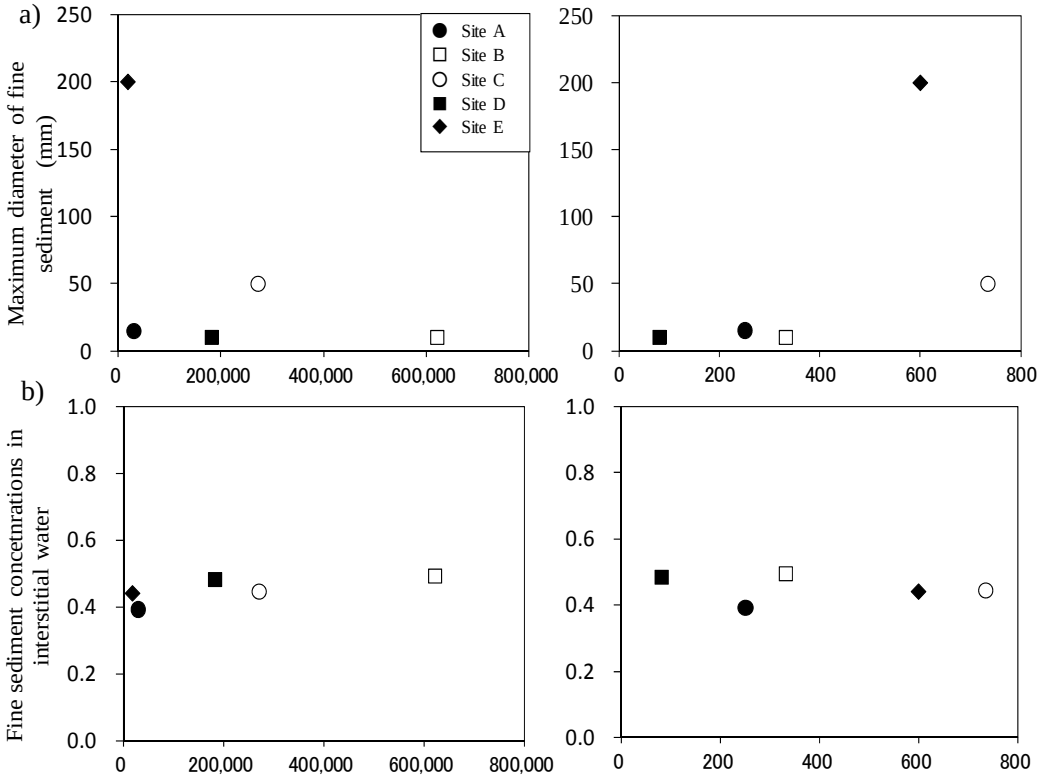

Fig.5 Factors controlling the phase-shift of fine sediment in debris flows. a) Relationship between the maximum diameter of fine sediment and the total volume and average particle diameter of debris flow, and b) relationship between the fine sediment concentration in interstitial water and the total volume, average particle diameter of debris flow

We calculated the fine sediment concentration in the interstitial water by averaging the simulated values of the 1/4, 1/2, and 3/4 points of the debris flow travel distances. The calculated fine sediment concentration in the interstitial water for the five debris flows was around 0.4–0.5. The best-fit D_c varied considerably among the debris flows, ranging from 8–200 mm and no correlations between D_c, the volume of debris flow, and average particle diameter of the sediment in the debris flow were found (Fig.5). However, the variation in the volumetric fine sediment concentration in the interstitial water was low, between 0.4–0.5, regardless of the variation of D_c, the volume of the debris flow, or grain size distribution (Fig.5).

We compiled previously published data relating to the fine sediment concentration of debris flows in Table 4. We included data from both debris flow flume experiments using fine sediment and field observations of viscous-type debris flows and volcanic mudflows. The upper limits of the fine sediment concentrations in the debris flow flume experiments ranged between 0.23–0.54, with most values around from 0.4–0.45. The upper limits of the fine sediment concentrations in the debris flow filed observations ranged between 0.3–0.51, similar to the results of the flume experiments.

These values are comparable for the fine

Table 4 Fine sediment concentrations from previously published data (*: Cited phenomena are from the references)

Previous experiment	Phenomenon *	Concentration of fine sediment
Ashida et al., 1985	Hyperconcentrated flow	0.15–0.35
Ashida et al., 1986	Hyperconcentrated flow	0.16–0.23
Arai and Takahashi, 1986	Mud flow	0.1–0.42
O'Brien and Julien, 1988	Mud flow	0.1–0.45
J.Major and Pierson, 1992	Fine-grained slurries	0–0.54
Egashira et al., 1993	High concentrated sediment-laden flow	0.04–0.32
Takahashi and Kobayashi, 1993	Viscous-type debris flow	0.21–0.32
Mainali and Rajaratnam, 1994	High-concentration fluid flow	0.03–0.44
Coussot and Piau, 1995	Clay–sand–water mixtures	0–0.43
Arai and Takahashi, 1996	High-concentration mud flow	0.23/0.4
Takahashi et al., 1996	Debris flow	0–0.4
Previous field observations	**Case**	**Concentration of fine sediment**
Takahashi and Kobayashi, 1993	Viscous type debris flow at Jiang-jia Creek, China	0.2–0.3
Ishida et al., 2001	Volcanic mudflow at Mt. Usu, Japan	0.51
Nanri et al., 2009	Volcanic mudflow at Mt. Tokachi, Japan	0.4

sediment concentrations in the interstitial water in our simulation, ranging between 0.4–0.5.

If the fine sediment concentration in a fluid becomes very high, the fluid may not demonstrate turbulent flow due to the high friction and frequent collisions among sediment particles. In other words, there may be an upper limit of fine sediment concentration in debris flow of high-intensity turbulence. Our results suggested that because the amount of fine sediment and turbulence magnitude were both sufficiently high, the fine sediment concentrations in the five debris flows approached the upper limit of concentration, despite variable grain size distributions, topography, and debris flow volumes.

These results were supported by our previous studies [*Nishiguchi et al*., 2012], which showed that the amount of sediment smaller than 10 mm often approached almost 30% in debris flows triggered by large-scale landslides. Thus, if the magnitude of turbulence in the interstitial water becomes high, the concentration of the phase-shifted sediment in the interstitial water may approach the upper limit concentration (around 0.4–0.5).

In this study, we assumed that although the fine sediments behave as fluid phase in a debris flow, these sediments could behave as a solid immediately prior to deposition, so that both coarse and fine sediment would form the deposited layer. Thus, the sediment concentration in debris flow remained almost constant in time and space. Results of this study were dependent on this assumption. However, we consider that the deposition process may be rather more complex in fact and futures studies should be important for clarifying the dynamics and deposition process of phase-shifted sediment in more detail.

6. CONCLUDING REMARKS

Our aim was to develop a technique to simulate large-scale stony debris flows to determine the environmental conditions that control the maximum diameter of phase-shifted sediment.

We assessed the maximum diameter (D_c) of phase-shifted sediment for five large-scale debris flows, and the conclusions of this study can be summarized as follows:

- The best-fit value of D_c showed considerable variation, from 8–200 mm, but the calculated volume concentration of the fine sediment (phase-shifted sediment) using the best-fit D_c varied little, ranging from 0.4–0.5.
- The settling velocities of the best-fit D_c were lower than both the friction velocities of the debris flow and the turbulent velocities of the interstitial water. This supported our assessment that sediment particles smaller than D_c can be suspended and behave as a fluid.
- There was no correlation between D_c, the volume of the debris flow, and grain size distribution.
- The volumetric range of fine sediment concentration in the interstitial water corresponded with the upper limits of the results of fine sediment concentrations in debris flows in previous research.

Consequently, if the amount of fine sediment and turbulence magnitude were sufficiently high, the fine sediment concentration of interstitial water might approach the upper limit concentration, regardless of the scale of the debris flow and the grain size distribution.

ACKNOWLEDGMENTS: We thank representatives from Kumamoto Prefecture, Tokushima Prefecture, Miyazaki Prefecture and Kagoshima Prefecture for providing access to data and reports.

REFERENCES

Arai M. and Takahashi T. (1986): The mechanics of mud flow, Proceedings of the Japan Society of Civil Engineers. 375/II-6, pp. 69-77.

Arai M. and Takahashi T. (1996): A measurement method of fluctuation velocity of high concentration mud-flow and the experimental results, Annual of Disaster Prevention Research Institute, Kyoto University, Vol. 40, pp. 1033-1038.

Ashida K., Takahashi T. and Michiue M. (1983): Sediment-related disasters and the countermeasure in river, Morikita Printing Co, Ltd., p. 30.

Ashida K., Yamano K. and Kanda M. (1985): Study on hyper-concentrated flow (1)-Viscosity and fall velocity-, Annual of Disaster Prevention Research Institute, Kyoto University, Vol. 28 (B-2), pp. 367-377.

Ashida K., Yamano K. and Kanda M. (1986): Study on hyper-concentrated flow (2)-Mechanism of the flow-Annual of Disaster Prevention Research Institute, Kyoto University, Vol. 29 (B-2), pp. 361-375.

Coussot, P. and Piau J.M. (1995): The effect of an addition of force-free particles on the rheological properties of fine suspensions, Canadian Geotechnical Journal, Vol.32, pp. 263-270.

Egashira S., Ashida K., Tanonaka S. and Sato T. (1993): Characteristics of high concentrated sediment laden flow, Annual Journal of Hydraulic Engineering, Vol. 37, pp. 517-522.

Egashira S., Honda N. and Miyamoto K. (1998): Numerical simulation of debris flow at the Gamaharazawa in the Hime river basin, Annual Journal of Hydraulic Engineering, Vol.

42, pp. 919-924.

Egashira S. and Itou T. (2004): Numerical simulation of debris flow, Journal of Japan Society of Computational Fluid Dynamics, Vol. 12, No. 2, pp. 33-43.

Egashira S., Sato T. and Chishiro K. (1994): Effect of particle size on the flow structure of sand water mixture, Annual of Disaster Prevention Research Institute, Kyoto University, Vol. 37, B-2, pp. 359-369.

Hotta N., Miyamoto K., Suzuki M. and Ohta T. (1998): Pore-water pressure distribution of solid-water phase flow in a rolling mill, Journal of the Japan Society of Erosion Control Engineering, 50, No. 6, pp. 11-16.

Hiura, H., Kaibori, M., Suemine, A., Satofuka, Y., and Tsutsumi, D. (2004): Sediment-related disasters in Kisawa-Village and Kaminaka-Town in Tokushima Prefecture, Japan, induced by the heavy rainfall of Typhoon Namtheun in 2004, Journal of the Japan Society of Erosion Control Engineering, Vol. 57, No. 4, pp. 39-47.

Ishida T., Nakano K., Yamada T., Hashida K. and Mizoguchi M. (2001): Run-out, flood and deposit characteristics of mud flow generated from a volcanic eruption at Mt. Usu and the mechanism of damage to bridges, Proceedings of the 50th meeting of the Japan Society of Erosion Control Engineering, pp. 438-439.

Iverson, R.M. (1997): The physics of debris flows, Reviews of Geophysics, Vol. 35, No. 3, pp. 245-296.

Kagoshima Prefecture (2007): Report on development of sediment disaster information mutually informing system, Chapter 7 and 8, pp.7.1-8.35.

Mainali, A. and Rajaratnam, N. (1994): Experimental Study of Debris Flows. Journal of Hydraulic Engineering, Vol. 120, No. 1, pp. 104-123.

Major J.J and Pierson T.C. (1992): Debris flow rheology: Experimental analysis of fine-grained slurries, Water Resources Research, Vol. 28, No. 3, pp. 841-857.

Miyazaki Prefecture (2006): Report of the committee for countermeasure for sediment disaster at Wanitsuka mountain range, 69 pp.

Nakagawa H., Takahashi T., Satofuka Y., Tachikawa Y., Ichikawa Y., Yoshida Y. & Nakamura Y. (1998): Debris flow disasters at Harihara River, Izumi City, Kagoshima Prefecture, 1997, Annuals of Disaster Prevention Research Institute, Kyoto University, Vol. 41 (B-2), pp. 287-298.

Nakatani K. (2010): Development and Application of debris flow numerical simulation system equipped with a graphical user interface, PhD Thesis, Kyoto University, 153 pp.

Nakatani, K., Satofuka, Y. and Mizuyama, T. (2007): Development of 'KANAKO', a wide use debris flow simulator equipped with GUI, Proceedings of 32nd Congress of IAHR, Venice, Italy, CD-ROM, 10 p, A2.c-182.

Nakatani, K., Wada, T., Satofuka, Y., Mizuyama, T. (2008): Development of "Kanako 2D (Ver.2.00)," a user-friendly one- and two-dimensional debris flow simulator equipped with a graphical user interface, International Journal of Erosion Control Engineering, Vol. 1, pp. 62-71.

Nanri T., Fukuma H., Harada N., Ando H., Itoh H., Hashinoki T. and Yamada T. (2009): Flow and sedimentation process of 1926 volcanic mudflow based on the field investigation data analysis, at Mt. Tokachi, Journal of the Japan Society of Erosion Control Engineering, Vol. 61, No. 5, pp. 21-30.

Nishiguchi, Y., Uchida, T., Tamura, K. and Satofuka, Y. (2011): Prediction of run-out process for a debris flow triggered by a deep rapid landslide, Italian Engineering Geology and Environment, Book, pp. 477-485.

Nishiguchi, Y. Uchida, T., Takezawa, N., Ishizuka, T. and Mizuyama, T. (2012): Run-out characteristics and grain size distribution of large-scale debris flows triggered by deep catastrophic landslides, International Journal of Erosion Control Engineering, Vol. 5, pp. 16-26.

Nishiguchi, Y., Uchida, T., Ishizuka, T., Satofuka, Y., Nakatani, K. (2013): Numerical simulation of debris flows induced by deep-seated catastrophic landslide, 12th International Symposium on River Sedimentation, pp. 119-127.

O'Brien, J.S. and Julien, P.Y. (1988): Laboratory analysis of mudflow properties, Journal of Hydraulic Engineering, Vol. 114, pp. 877-887.

Rubey W.W. (1933): Settling velocities of gravel, sand and silt particles, American Journal of Science, Vol. 25, pp. 325-338.

Takahashi T. (1977): Mechanism of occurrence of mud-debris flows and their characteristics in motion, Annual of Disaster Prevention Research Institute, Kyoto University, Vol. 20, B-2, pp. 405-435.

Takahashi T. (2004): Mechanics and countermeasure of debris flow, Kinmirai-sha, 432 pp.

Takahashi T. and Kobayashi K. (1993): Mechanics of the viscous type debris flow, Annual of Disaster Prevention Research Institute, Kyoto University, Vol. 36 (B-2), pp. 433-449.

Takahashi T., Satofuka Y. and Chishiro K. (1996): Mechanical law of debris flows in inertial regime, Annual of Disaster Prevention Research Institute, Kyoto University, Vol. 39 (B-2), pp. 333-346.

Takezawa N., Uchida T., Suzuki R., and Tamura K. (2009): Estimation of debris flow induced by a deep-seated landslide at the Funaishi river basin, Kagoshima Prefecture in Japan, Journal of the Japan Society of Erosion Control Engineering, Vol. 62, No. 2, pp. 21-28.

Uchida, T., Nishiguchi, Y., Nakatani, K., Satofuka, Y., Yamakoshi, T., Okamoto, A. and Mizuyama, T. (2013): New Numerical Simulation Procedure for Large-scale Debris Flows (Kanako-LS), International Journal of Erosion Control Engineering, Vol. 6, pp. 58-67.